THREE-DIMENSIONAL SIMULATION OF CONTROLLED COOLING OF ELECTRONIC COMPONENT BY NATURAL AND MIXED CONVECTION

by

Lahoucine BELARCHE*, Btissam ABOURIDA, Hicham DOGHMI, Mohamed SANNAD, and Meryem OUZAOUIT

National School of Applied Sciences, Ibn Zohr University, Agadir, Morocco

Original scientific paper
https://doi.org/10.2298/TSCI190508181B

The present study is the 3-D simulation of cooling control of electronic component, by natural convection and mixed convection in a cubical enclosure, filled with air. The heating square portion similar to the integrated electronic device and releasing a constant flux is placed on the right vertical wall of the enclosure. The same wall has, in its upper part, an extractor, while the rest of the considered wall is adiabatic. Its opposite wall has an opening maintained at a cold temperature. For low temperatures, the cooling of the component is provided by natural convection, however, in the case of strong temperature gradients, the extractor, operating at variable velocity, allows the evacuation of the dissipated heat. The cooling control of the component, the temperature distribution as well as the flow of fluid in the cavity is studied according to the governing parameters, namely the Rayleigh and Reynolds numbers. The obtained results show that the control cooling of the electronic components has a great industrial interest compared to the continuous cooling (ventilation), by an optimal choice of the governing parameters and the material constituting the components.

Key words: *3-D natural convection, 3-D mixed convection, electronic components, numerical simulation*

Introduction

Currently, electronic systems are becoming more and more efficient. As a result, the heat flux generated by these systems is constantly increasing. This heat must be removed to prevent premature failure of the components and the electronic systems. The manufacturers provide the maximum temperatures below which devices can operate optimally, however, the internal temperature of the controlled unit exceeds the specifications specified by the manufacturer. The case cooling units are useful for extracting heat from the electronic housings. Several methods of housing cooling are currently used. Some devices use natural convection cooling while others use forced convection. For the choice of the optimal mode to use, a study is necessary to determine the structure of the fluid-flow, the distribution of the temperature field, and the heat transfer rates. Among the means of study of heat transfer phenomena, the experimental route seems the least developed despite the relevant information it can offer this is due to the difficulties of implementation related to the control of different parameters and the high cost. These technical and material problems have largely contributed to the develop-

* Corresponding author, e-mail: l.belarche@uiz.ac.ma

ment of mathematical models and the development of numerical codes and analytical methods. Although the latter are less expensive, they are however the least used because of the limitation of the cases where they can be applied. The advantage of numerical modeling lies in the possibility of performing parametric studies and thus obtaining reliable results, generally comparable with experimental laboratory tests. Meanwhile, and despite the extraordinary advances made by computer technology, the numerical resolution of heat transfer equations requires cautious and progressive approaches.

Some authors have been interested in the problem of natural convection heat transfer in enclosures. A comprehensive review of this topic is given by Bejan and Kraus [1] and Goldstein *et al.* [2] for different combinations of geometrical and thermal imposed conditions. However, in most of these works, the studied configurations are 2-D cavities, partially heated, with one or more heating portions [3, 4]. However, it should be noted that the majority of the available works deal with the case of 2-D convection, whereas the 3-D natural convection [5-7] approach allows a better, more realistic simulation of the flow and heat transfer within the cavity.

Other authors have conducted studies of mixed convection, hence, many authors [8-18] have reported their studies of the 2-D laminar mixed convection. Their principal results showed that the interaction between the natural convection and the external forced convection plays a simultaneous role in the heat removal. The ventilated cavities have been studied numerically by the authors in references [19-28] for different inlet-outlet opening positions. They found that the increase of the thermal parameters or (and) the optimal choice of the ventilation orientations can lead to the best cooling effectiveness. The 3-D mixed convection inside an open cavity has been studied numerically by Stiriba *et al.* [29]. Their results showed that the flow motion becomes unsteady with Kelvin-Helmholtz instabilities at the shear layer and the heat transfer rate increases significantly for Reynolds number and Grashof number. A numerical comparison of the 3-D and 2-D mixed convection phenomenon inside an air-cooled cavity was conducted by Moraga and Lopez [30]. They observed a major difference between the global Nusselt numbers calculated from the 2-D and the 3-D models. The 3-D model allowed the visualization of the flow structure and the estimation of the heat transfer rate. A recent 3-D numerical investigation of the inlet opening effect on the mixed convection inside a 3-D ventilated cavity was presented by Doghmi *et al*. [31]. They found that the average Nusselt number at the active walls increases with increasing Richardson numbers and the heat transfer rate increase and decrease at the hot and cold wall respectively by increasing the inlet opening section. Very recently the same authors [32] studied numerically the mixed convection heat transfer inside a partially heated 3-D ventilated cavity. The authors showed that heat transfer rate increases with decreasing the heating section dimensions for fixed Reynolds and Richardson numbers.

Thus, the objective of this study is to numerically study the natural and mixed convection within a 3-D cavity with an electronic component located on the vertical surface of the cavity and is modeled by a square surface supplying a constant heat flux. The opposite wall has an opening maintained at a cold temperature. In the context of this study, we will be interested in verifying whether natural convection can ensure the cooling of the component, then, in the second case of mixed convection, to determine the optimal Reynolds number allowing cooling while protecting the component and to guarantee the reliability of the electronic system numbers.

Physical problem and governing equations

The schematic configuration of the considered 3-D cubical cavity co-ordinates and boundary conditions are shown in fig. 1. It consists of a cubical 3-D cavity ($H = L = B$), with square heating section with relative side, $\varepsilon = D/L$, placed on the right vertical wall and submitted to constant heat flux density, q''. The rest of the same wall is adiabatic. For low temperatures, the component is cooled by circulating air, fig. 1(a), in contact with an inlet opening of rectangular section of relative height, $\lambda = h/H$, which maintained at a cold ambient temperature, T_C. In the case of strong temperature gradients, the extractor with relative side $\gamma = A/H$, located on the top of the right vertical wall and operating at variable velocity, allows the evacuation of the dissipated heat, fig. 1(b). The rest of the same wall is adiabatic. The other four walls of the cavity are maintained adiabatic too.

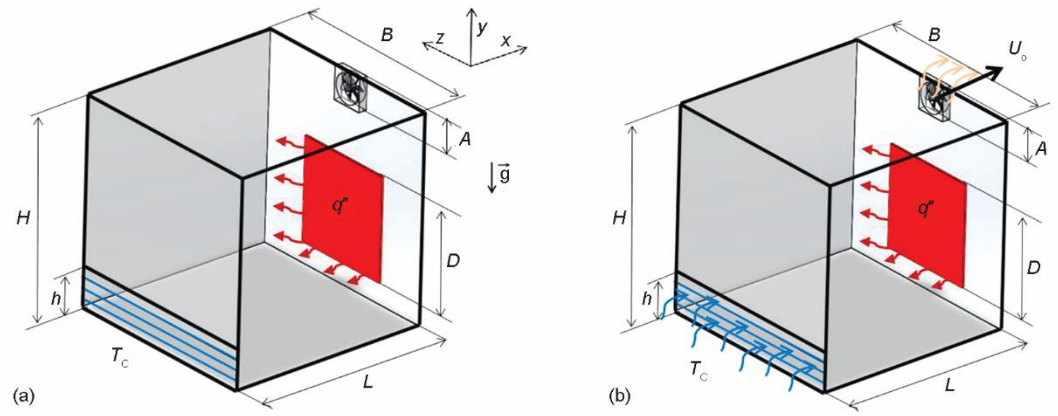

Figure 1. Studied configuration and co-ordinates; (a) Mode 1 (natural convection) and (b) Mode 2 (mixed convection)

The flow is considered to be 3-D, laminar, Newtonian, and incompressible. The thermophysical properties of the fluid are assumed constant except for the density in the expression of the buoyancy force of the motion equation in the vertical direction, using the Boussinesq approximation. Viscous dissipation in the energy equation is neglected. The working fluid is assumed to be air (Pr = 0.71). Considering the aforementioned assumptions, the governing equations for the 3-D laminar incompressible fluid are expressed in the following dimensionless form:

– Continuity equation

$$\frac{\partial U}{\partial X}+\frac{\partial V}{\partial Y}+\frac{\partial W}{\partial Z}=0 \tag{1}$$

– Moment equation on X

$$\frac{\partial U}{\partial \tau}+\frac{\partial (UU)}{\partial X}+\frac{\partial (VU)}{\partial Y}+\frac{\partial (WU)}{\partial Z}=-\frac{\partial (P)}{\partial X}+\Gamma_1\left(\frac{\partial^2 U}{\partial X^2}+\frac{\partial^2 U}{\partial Y^2}+\frac{\partial^2 U}{\partial Z^2}\right) \tag{2}$$

– Moment equation on Y

$$\frac{\partial V}{\partial \tau}+\frac{\partial (UV)}{\partial X}+\frac{\partial (VV)}{\partial Y}+\frac{\partial (WV)}{\partial Z}=-\frac{\partial (P)}{\partial Y}+Se\theta+\Gamma_1\left(\frac{\partial^2 V}{\partial X^2}+\frac{\partial^2 V}{\partial Y^2}+\frac{\partial^2 V}{\partial Z^2}\right) \tag{3}$$

– Moment equation on Z

$$\frac{\partial W}{\partial \tau}+\frac{\partial (UW)}{\partial X}+\frac{\partial (VW)}{\partial Y}+\frac{\partial (WW)}{\partial Z}=-\frac{\partial (P)}{\partial Z}+\Gamma_1\left(\frac{\partial^2 W}{\partial X^2}+\frac{\partial^2 W}{\partial Y^2}+\frac{\partial^2 W}{\partial Z^2}\right) \tag{4}$$

– Equation of energy

$$\frac{\partial \theta}{\partial \tau}+\frac{\partial (U\theta)}{\partial X}+\frac{\partial (V\theta)}{\partial Y}+\frac{\partial (W\theta)}{\partial Z}=\Gamma_2\left(\frac{\partial^2 \theta}{\partial X^2}+\frac{\partial^2 \theta}{\partial Y^2}+\frac{\partial^2 \theta}{\partial Z^2}\right) \tag{5}$$

where U, V, and W are the velocity components in the X-, Y-, and Z-directions, respectively, P – the pressure, τ – the time, and θ – the temperature. The non-dimensional variables used in these equations are defined by:

$$(X,Y,Z)=\left(\frac{X}{H},\frac{Y}{H},\frac{Z}{H}\right),\quad (U,V,W)=\left(\frac{uH}{\alpha},\frac{vH}{\alpha},\frac{wH}{\alpha}\right),\quad \theta=\frac{T-T_\mathrm{C}}{q''H}k$$

$$\tau=\frac{\alpha}{H^2}t \quad \text{and} \quad P=\frac{p-p_0}{\rho_0 u_0} \tag{6}$$

The parameters, Γ_1, Se, and Γ_2 according to the considered mode are expressed in the tab. 1.

Table 1. Parameters expressions

	Γ_1	Se	Γ_2
Mode 1	Pr	RaPr	1
Mode 2	Re^{-1}	$\mathrm{RaPr}^{-1}\mathrm{Re}^{-2}$	$(\mathrm{RePr})^{-1}$

The dimensionless numbers observed in tab. 1, Re, Ra, and Pr, are the numbers of Reynolds, Rayleigh, and Prandtl, respectively. They are defined:

$$\mathrm{Re}=\frac{Hu_0}{\nu},\quad \mathrm{Ra}=\frac{\mathrm{g}\beta q'' H^4}{\alpha\nu k} \quad \text{and} \quad \mathrm{Pr}=\frac{\nu}{\alpha} \tag{7}$$

where β, ν, k, and α are thermal expansion coefficient, kinematic viscosity, thermal conductivity, and thermal diffusivity, respectively.

The boundary conditions used in this study are given in dimensionless form as follows.

– $U = V = W = 0$ on the rigid walls of the enclosure,
– the vertical walls ($Z = 0$ and $Z = 1$) and horizontal walls ($Y = 0$ and $Y = 1$): $\partial\theta/\partial n = 0$ (n is the normal direction to the considered wall),
– vertical right wall: $\partial\theta/\partial X = -1$ through the component and $\partial\theta/\partial X = 0$ elsewhere on the wall,
– vertical left wall: $\theta_\mathrm{C} = 0$ at the opening and $\partial\theta/\partial X = 0$ elsewhere on the wall,
– in the case of natural convection: $U = V = W = 0$ at the extractor and at the opening, and
– in the case of mixed convection: $U = 1$ and $V = W = 0$ at the extractor and $\partial U/\partial X = 0$ at the opening.

The local Nusselt number and the average Nusselt number calculated on the component are respectively defined at each time step by:

$$\mathrm{Nu}(X,Z,\tau)=\frac{q''H}{[T(y,z,t)_{x=1}-T_\mathrm{C}]k}=\frac{1}{\theta(Y,Z,\tau)_{X=1}} \tag{8}$$

$$\mathrm{Nu}(\tau)=\frac{1}{\varepsilon^2}\int \mathrm{Nu}(X,Z,\tau)\,\mathrm{d}Y\mathrm{d}Z \tag{9}$$

where θ (Y, Z, τ), in eq. (8), is the local dimensionless temperature at a given point of the component surface.

Numerical method

The Navier-Stokes and energy equations are solved by the home developed FORTRAN code using the finite volume method developed by Patankar [33] adopting the power law scheme. To overcome the difficulty associated with the determination of the pressure, we suggest solving the equations of conservation of momentum coupled with the continuity equation using SIMPLEC algorithm (the Semi-Implicit Method for Pressure Linked Equations Consistent). To solve the algebraic system obtained after discretization of PDE, the alternating direction implicit (ADI) scheme is used. The tri-diagonal system obtained in each direction is solved using the THOMAS algorithm. The convergence of the numerical code is established at each time step according to the following criterion, which fixes the relative difference between the field variables ϕ (= U, V, W, T, P), in successive time steps (n and n+1) less than 10^{-5}:

$$\sum_{i,j,k=1}^{i\max,j\max,k\max}\frac{\left|\phi_{i,j,k}^{n+1}-\phi_{i,j,k}^{n}\right|}{\left|\phi_{i,j,k}^{n}\right|}\le 10^{-5} \tag{10}$$

where i, j, and k are the grid positions.

To check the effect of the grid size on the fluid-flow and heat transfer, preliminary tests were conducted for different combinations of the governing parameters. Finally, the non-uniform grid of 81 × 81 × 81 nodes was estimated to be appropriate for the present study since it permits a good compromise between the computational cost (a significant reduction of the execution time) and the accuracy of the obtained results. The optimal time step was also found to be equal to 10^{-4} after multiple tests.

Finally, the accuracy of the currently developed numerical code was checked by comparing its results with those obtained, firstly, in the case of 3-D natural convection heat transfer and secondly, in the case of 3-D mixed convection heat transfer. Thus our results are compared to those presented by Fusegi *et al.* [6] and Frederic and Quiroz [7] in the case of cubical enclosure with a partially heated wall (s/L = 0.3). A comparison of the averaged Nusselt number, Nu, and maximum values velocities U and V, in the mid-plane Z = 0.5 is given in tab. 2 for Ra = 10^6. The obtained results show excellent agreement with the two references, with maximum differences not exceeding 1.55% for Nu, 1.1% and 0.88% respectively for $U_{\max}$ and $V_{\max}$ comparing to Fusegi's [6] results and 1.23% for Nu, 0.204% and 1.04%, respectively, for $U_{\max}$ and $V_{\max}$ comparing to Frederic's [7] result .

In addition, the code was validated in the case of 3-D mixed convection heat transfer in a ventilated cavity with studies of Moraga and Lopez [30] in terms of velocity at Z = 0.5 and Y = 0.5 shown in fig. 2 for Reynolds number, Re = 10 and Richardson number, Ri = 10.

Table 2. Validation of the numerical code with published results in terms of Nu, U_{max} and V_{max} for Ra =10^6

	Nu	U_{max}	V_{max}
[6]	8.77	0.08416	0.2922
Present work	8.906	0.08508	0.2948
Difference [%]	1.55	1.1	0.88
[7]	3.4857	58.3830	151.693
Present work	3.5286	58.5024	153.27
Difference (%)	1.23	0.204	1.04

It can be seen from this comparison that there is a good agreement between the present results and those presented by the mentioned references.

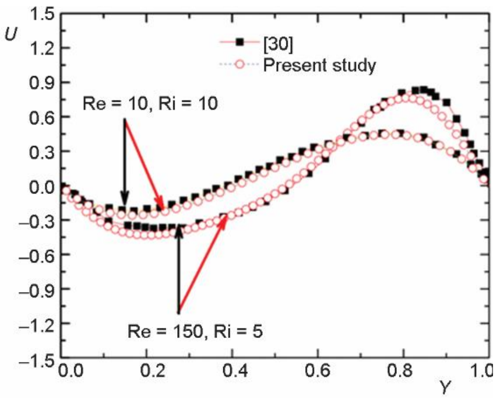

Figure 2. Comparison between *U* velocity component obtained at *X* = 0.75, *Z* = 0.5 and those presented by [30]

Results and discussion

Numerical computations are performed to analyze the maximum temperature reached by the electronic component and determine its position. The aim is to control the cooling by using the appropriate mode: natural convection or mixed convection, at low or high velocity, and then to improve the operating temperature of the electronic component by a local surface treatment while avoiding the total treatment that can cost too much. The isotherms at the component level, the position of the maximum temperature, and the hydrodynamic and thermal fields in the 3-D cavity are presented as a function of the governing parameters, namely the Rayleigh and the Reynolds numbers. The Prandtl number is fixed at 0.71, the height of the opening is fixed at 0.2, while the extractor and the component dimensions are 0.2 × 0.2 and 0.35 × 0.35, respectively.

Determinations the optimum Reynolds number

The cooling mode of the component is based on the maximum temperature reached at that component. The operating temperature is set at a value θ_o, given by the manufacturer, not to be exceeded. As long as the maximum temperature θ_{max} remains below 50% of the value θ_o, natural convection ensures cooling. If the temperature exceeds 50% of θ_o, the air extractor will be triggered and operate at a low speed corresponding to a number of Reynolds, Re_1. If the temperature exceeds 60% of θ_o, the speed of the extractor increases and thus works with an optimal Reynolds number which is determined for Ra = 10^3 corresponds to the most critical case where the component reaches the maximum temperature values. The two temperatures corresponding to 50% of θ_o and 60% of θ_o are chosen for the tripping of the extractor instead of θ_o to avoid the effect of thermal inertia and the negative effect of the mixed convection. This last effect corresponds to the hot air trapped on the component, a phenomenon similar to that reported by Manca *et al.* [14]. Noting that to determine Re_o allowing cooling while protecting the component, as shown in fig. 3, we increase Re_2 by steps of 100. Hence, the extractor will be operating with these two Reynolds numbers: Re_1 and Re_o for all studied Rayleigh numbers. In our case, we consider $Re_1 = 100$ and $Re_o = 1000$.

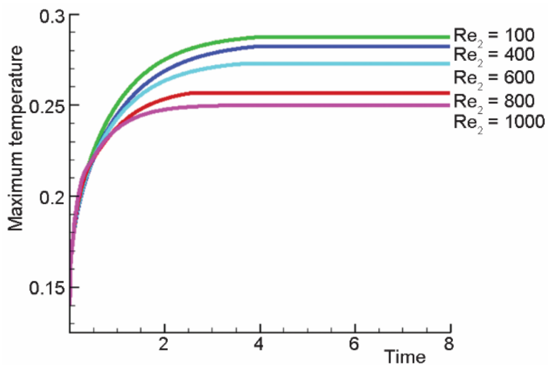

Figure 3. Maximum temperature θ_{max} for different Re_2

Effect of the Rayleigh number on cooling mode

To illustrate the effect of the Rayleigh number (Ra = 10^3-10^6) on cooling mode, we present in figs. 4(a)-4(d), the temporal evolutions of the maximum temperature, its position and the Reynolds number in action. The numerical results are reported in tab. 3.

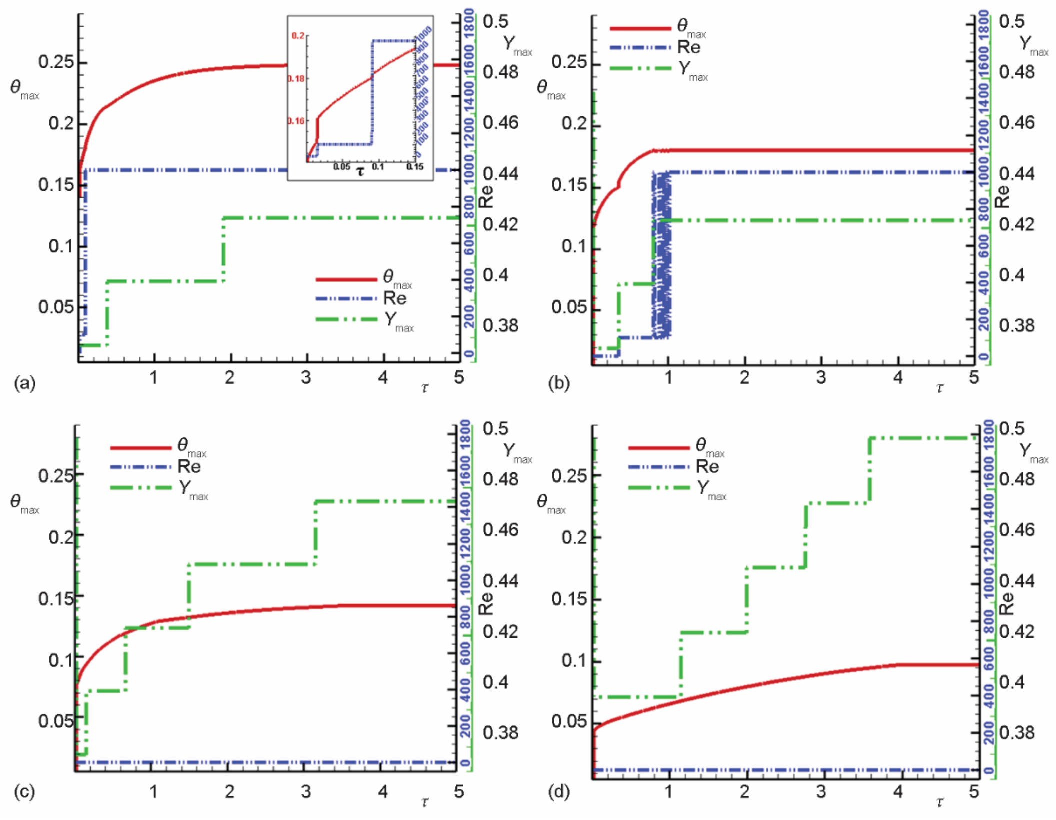

Figure 4. Temporal evolutions of the maximum temperature, its position and the Reynolds number for: (a) Ra = 10^3, (b) Ra = 10^4, (c) Ra = 10^5, and (d) Ra = 10^6

Table 3. Mode in action, intensity (Ψ_{max}, Ψ_{min}), maximum temperature θ_{max} and its position Y_{max} for Ra = 10^3-10^6

Ra	Time	Mode	Re	Mode duration	ψ_{max}	ψ_{min}	θ_{max}	Y_{max}
10^3	$\tau = 0.015 \leq 0.016$	1	0	0.016	0.0098	– 0.0017	0.1496	0.3718
	$0.016 \leq \tau = 0.08 \leq 0.093$	2	100	0.077	0. 5467	– 0.0059	0.1780	0.3718
	$0.093 \leq \tau = 1$	2	1000	≥ 0.093	0.7738	– 0.0389	0.2353	0.3974
10^4	$\tau = 0.2 \leq 0.349$	1	0	0.349	0.0265	– 0.0045	0.1374	0.3718
	$0.349 \leq \tau = 0.5 \leq 0.803$	2	100	0.454	0. 5624	– 0.0060	0.1684	0.3974
	$1.016 \leq \tau = 2$	2	1000	≥ 1.016	0.7941	– 0.0177	0.1805	0.4487
10^5	$\tau = 0.1$	1	0	–	0.01973	– 0.0024	0.0888	0.3718
	$\tau = 1$	1	0		0. 0585	– 0.0086	0.1269	0.4231
	$\tau = 2.4$	1	0		0.0785	– 0.0131	0.1377	0.4487
10^6	$\tau = 0.1$	1	0	–	0.01032	– 0.00112	0.0482	0.3718
	$\tau = 2.4$	1	0		0. 0530	– 0.0064	0.0661	0.3974
	$\tau = 4$	1	0		0.0826	– 0.0104	0.0841	0.3974

The component cooling principle is represented in fig. 4(a) for a Rayleigh number Ra = 10^3 and an operating temperature θ_o set at 0.25. Hence, fig. 4(a) represents the evolution of the maximum temperature θ_{max} reached at the component level, the mode in action and the position Y_{max} of this maximum temperature. Figure 4(a) and tab. 3 show that at the beginning and during a period $\tau = 1.6 \cdot 10^{-2}$ where the maximum temperature θ_{max} remains below 50% of θ_o, the mode in action is natural convection. When the maximum temperature $\theta_{max} = 0.125$ corresponding to 50% of θ_o, reached at $\tau = 1.6 \cdot 10^{-2}$, the extractor is triggered and operates with a Reynolds number Re = 100. The θ_{max} increases more and exceeds 60% of θ_o. The extractor operates at the optimum speed ($Re_o = 1000$) making it possible to set θ_{max}, in steady-state, at a value of $0.248 \leq \theta_o = 0.25$.

For Ra = 10^4, fig. 4(b) and tab. 3 show that the cooling of the component is similar to the case where Ra = 10^3. It is carried out in three phases but with an increase of durations: the cooling by natural convection duration $\tau = 0.349$ followed by cooling by mixed convection with small speed of duration $\tau = 0.454$ and beyond $\tau = 1.016$, the extractor works with a high speed to evacuate excess heat. For Ra $\geq 10^5$, fig. 4(c) (Ra = 10^5), fig. 4(d) (Ra = 10^6) and tab. 3 show that natural convection remains the only cooling mode of the component. Therefore, depending on the Rayleigh number, natural convection alone can provide cooling. However for some Rayleigh numbers, either mixed convection with low speed or high speed is mandatory. This explains the interest of using a controlled extractor over another one operating continuously.

Isotherms and streamlines

In order to visualize the flow and the temperature distribution within the studied configuration, streamlines (a) and isotherms in the plane $Z = 0.5$ (b) as well as isotherms on the heating section (c) are, respectively, shown in figs. 5(A)-5(D), for $\varepsilon = 0.35$ and for Ra = 10^3-10^6.

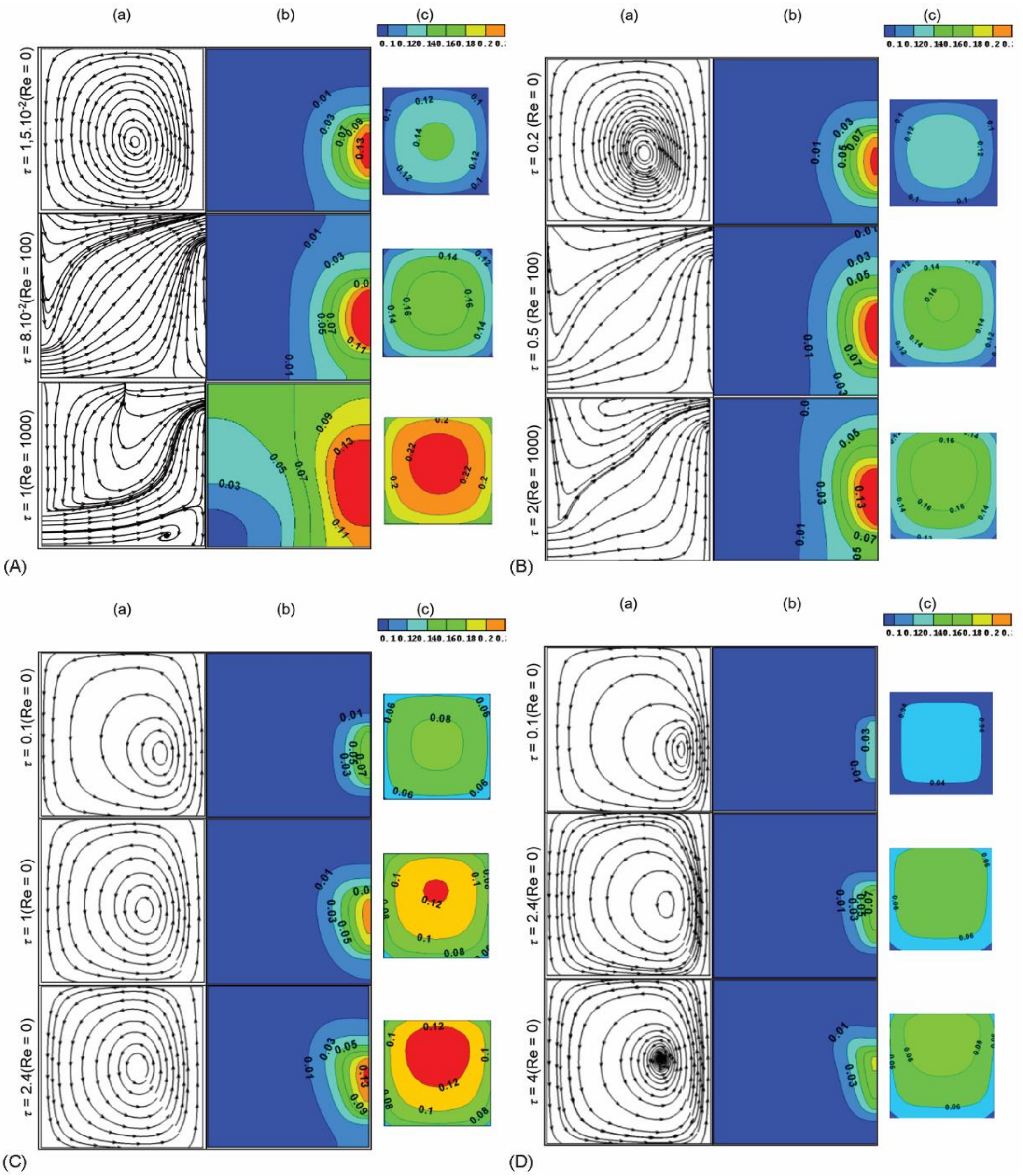

Figure 5. (A) Streamlines (a) isotherms (b) at Z = 0.5 and isotherms on the heated section (c) for Ra = 10^3 and different Re; (B) streamlines (a) isotherms, (b) at Z = 0.5 and isotherms on the heated section, (c) for Ra = 10^4 and different Re; (C) streamlines (a) isotherms, (b) at Z = 0.5 and isotherms on the heated section, (c) for Ra = 10^5 and Re = 0; and (D) streamlines (a) isotherms, (b) at Z = 0.5 and isotherms on the heated section, (c) for Ra = 10^6 and Re = 0

For Ra = 10^3-10^4, the cooling of the component is carried out in three phases: cooling by natural convection of duration $\tau = 1.6\cdot10^{-2}$ for Ra = 10^3 (τ = 0.349 for Ra = 10^4), in this phase, as shown in figs. 5(A), 5(B), and tab. 3, the flow is formed of a single cell occupying the entire cavity, rotating in the trigonometric direction with a low intensity (ψ_{max} = 0.0098 for Ra = 10^3 and ψ_{max} = 0.0265 for Ra = 10^4). The fluid is heated in contact with the component placed on the right wall of the cavity and upwards to finally give up heat to the vertical wall at the opening maintained at a cold temperature, θ_C = 0. The maximum temperature (θ_{max} = 0.1496 for Ra = 10^3 and θ_{max} = 0.1374 for Ra = 10^4) is reached at the position Y_{max} = 0.3718 for Ra = 10^3 and Ra = 10^4. In the second phase where the cooling is provided by the mixed convection with the small speed of duration $\tau = 7.7\cdot10^{-2}$ for Ra = 10^3 (τ = 0.454 for Ra = 10^4), the cold fluid entering the opening moves towards the outlet carrying heat from the component warm with medium intensity (ψ_{max} = 0.5467 for Ra = 10^3 and ψ_{max} = 0.7941 for Ra = 10^4). The maximum temperature (θ_{max} = 0.1780 for Ra = 10^3 and θ_{max} = 0.1684 for Ra = 10^4) is reached at the position Y_{max} = 0.3718 for Ra = 10^3 and Y_{max} = 0.3947 for Ra = 10^4. For the third phase ($\tau \geq 9.3\cdot10^{-2}$ for Ra = 10^3 and $\tau \geq 1.016$ for Ra = 10^4), the flow intensifies (ψ_{max} = 0.7738 for Ra = 10^3 and ψ_{max} = 0.7941 for Ra = 10^4) with the appearance of a re-circulation flow near the lower wall. The maximum temperature (θ_{max}= 0.2353for Ra = 10^3 and θ_{max} = 0.1805 for Ra = 10^4) is reached at the position Y_{max} = 0.3974 for Ra = 10^3 and Y_{max} = 0.4487 for Ra = 10^4.

For Ra = 10^5-10^6, as shown in figs. 5(C), 5(D), and tab. 3, the cooling of the component is carried out only by natural convection: the flow is formed of a single cell occupying the entire cavity, rotating in the trigonometric direction whose core is located near the component which moves towards the left. This displacement is accompanied by an increase in intensity as shown in tab. 3. The maximum temperatures are low compared to the case Ra = 10^3-10^4 whose positions are between 0.3718 and 0.4487.

Maximum temperature position

Depending if the objective is to increase the operating temperature or instead to save the material in which the component is made of, the determination of the maximum temperature position, Y_{max} is always necessary. Figures 5(A)-5(D), and tab. 3 show that for all the considered Rayleigh numbers, the maximum temperature is located in the Z = 0.5 plane. This is due to the symmetry of the geometry and the thermal boundary conditions. Thus, the position of θ_{max} depends only on Y. The presented figures and table show that in general, for all the considered Rayleigh numbers, the maximum temperatures θ_{max} are located near the centers of these sections (Y = 0.3974). Note that θ_{max} is reached for Ra = 10^3 at position (X = 1, $0.37184 \leq Y \leq 0.3974$, Z = 0.5). Therefore, the intervention to be adopted must be done in this position. Hence, if we want to increase the operating temperature, we can act on the area (X = 1, $0.37184 \leq Y \leq 0.3974$, Z = 0.5) with the same amount of material used for to the whole component. However, if we want a material's gain, we can act specifically on the area (X = 1, $0.37184 \leq Y \leq 0.3974$, Z = 0.5) using locally the quantity of material allowing a good functioning of the component and the appropriate resistance at the same temperature. This can be a good alternative if we want to reduce the cost of the component's treatment, which can be very high in some specific applications.

Heat transfer

In order to analyze the heat transfer performance for the studied configuration, we present on fig. 6 the temporal evolution of the average Nusselt numbers, Nu(τ), calculated on the component surface and for different Rayleigh numbers.

Figure 6 shows that at the beginning of the operation, where the natural convection is the cooling mode, the heat transfer reaches their maximum values, tab. 4, for all the Rayleigh numbers studied. For Ra = 10^5-10^6, these maximum values are very significant because the heat transfer is dominated by natural convection [Nu (τ = 10^{-4}) = 340.72 for Ra = 10^5 and Nu (τ = 10^{-4}) = 369.17 for Ra = 10^6]. For Ra = 10^3-10^4, the maximum value of Nu (τ): Nu (τ = 10^{-4}) = 9.39 for Ra = 10^3 is justified by the heat transfer that is dominated by the conduction. For each fixed Rayleigh number, Nu (τ) decreases very rapidly for low τ. As τ increases, the Nusselt number gradually decreases to reach the established regime to maintain the maximum temperature below the operating temperature. This regime is obtained by only natural convection for Ra = 10^5-10^6 and by mixed convection (Re = 10^3) for Ra = 10^3-10^4.

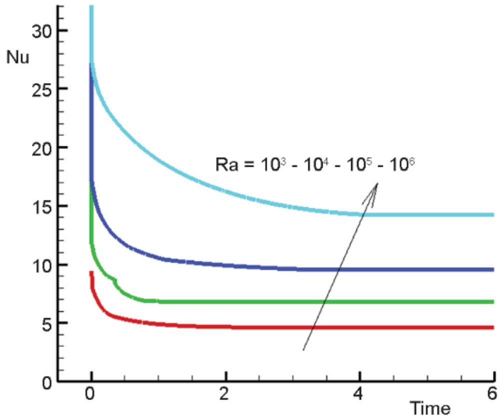

Figure 6. Temporal evolution of the average Nusselt numbers for Ra =10^3-10^6

Table 4. Average Nusselt numbers at the first step time and regime established for Ra = 10^3-10^6

	First step time τ = 10^{-4}		Regime established	
Ra	Mode	Nu	Mode	Nu
10^3	1	9.391520	2 (Re = 10^3)	4.605338
10^4	1	281.9569	2 (Re = 10^3)	6.837043
10^5	1	340.7224	1 (Re = 0)	9.549717
10^6	1	369.1702	1 (Re = 0)	14.26147

Conclusions

A numerical study was performed to investigate the electronic components, controlled cooling, which has a great industrial interest compared to the continuous cooling (ventilation). The main conclusions of the present study can be summarized as follows.

- The optimal Reynolds number allowing cooling was determined, Re_o = 10^3 for Ra = 10^3.
- For Ra = 10^5-10^6, the cooling of the component is carried out only by natural convection, while for Ra = 10^3-10^4, the mixed convection with Re = 1000 is necessary.
- The maximum temperatures are reached for Ra = 10^3 at the position (X = 1, 0.3718 ≤ Y ≤ 0.3974, Z = 0.5) .
- For each fixed Rayleigh number, the average Nusselt number, Nu(τ), decreases very rapidly with the time τ. As τ increases, the Nusselt number gradually decreases to reach the established regime in order to maintain the maximum temperature below the operating temperature.

Nomenclature

A	– side of the extractor, [m]	H	– height of the cavity, [m]
B	– depth of the cavity, [m]	h	– height of the openings, [m]
D	– length of the square heating section, [m]	k	– thermal conductivity, [$Wm^{-1}K^{-1}$]
g	– gravitational acceleration, [ms^{-2}]	L	– cavity length, [m]

Nu – Nusselt number
Pr – Prandtl number ($=\nu/\alpha$)
P – non-dimensional pressure
p – pressure, [Nm^{-2}]
q'' – heat flux, [Wm^{-2}]
Ra – Rayleigh number [$=g\beta q''H^4/(\nu\alpha k)$]
Re – Reynolds number
Ri – Richardson number
T – temperature
T_c – ambient temperature
t – time
u, v, w – dimensional velocities, [ms^{-2}]
U, V, W – dimensionless velocities

Greek symbols

α – thermal diffusivity, [$\mathrm{m}^2\mathrm{s}^{-1}$]
β – volumetric thermal expansion coefficient, [K^{-1}]
γ – non-dimensional side of the extractor
ε – non-dimensional side of the square hot section
θ – non-dimensional temperature
λ – non-dimensional height of the openings
μ – dynamic viscosity, [$\mathrm{kgm}^{-1}\mathrm{s}^{-1}$]
ρ – density, [kgm^{-3}]
τ – non-dimensional time
ν – kinematic viscosity, [$\mathrm{m}^2\mathrm{s}^{-1}$]
ψ – streamline intensity

Subscripts

C – cold
max – maximum value
o – operating value

References

[1] Bejan, A., Kraus, A. D, *Heat Transfer Handbook*, John Wiley, New York, USA, 2003
[2] Goldstein, R. J., *et al.*, A review of 2003 literature, *Int. J. of Heat and Mass Transfer*, *49* (2006), 3-4, pp. 451-534
[3] Sharif, M. A. R., Mohammad, T. R., Natural Convection in Cavities with Constant Flux Heating at the Bottom Wall and Isothermal Cooling from the Sidewalls, *Int. J. Therm. Sci*., *44* (2005), 9, pp. 865-878
[4] Ben Cheikh, N., *et al*., Influence of Thermal Boundary Conditions on Natural Convection in a Square Enclosure Partially Heated from Below, *Int. J. Heat and Mass Transfer*, *34* (2007), 3, pp. 369-379
[5] Ben-Cheikh, N., *et al*., Three-Dimensional Study of Heat and Fluid-flow of Air and Dielectric Liquids Filling Containers Partially Heated from Below and Entirely Cooled from Above, *Int. J. Heat Transfer*, *37* (2010), 5, pp. 449-456
[6] Fusegi, T., *et al*., A Numerical Study of Three-Dimensional Natural-Convection in a Differentially Heated Cubical Enclosure, *Int. J. Heat Mass Transfer*, *34* (1991), 6, pp. 1543-1557
[7] Frederick, R. L., Quiroz, F., On the Transition from Conduction to Convection Regime in a Cubical Enclosure with a Partially Heated Wall, *Int. J. Heat Transfer*, *44* (2001), 9, pp. 1699-1709
[8] Papanicolaou, E., Jaluria, Y., Mixed Convection from a Localized Heat Source in a Cavity with Conducting Walls: A Numerical Study, *Numerical Heat Transfer, Part A Applications*, *23* (1993), 4, pp. 463-484
[9] Yücel, C., *et al*., Mixed Convection Heat Transfer in Open Ended Inclined Channels with Discrete Isothermal Heating, *Numerical Heat Transfer, Part A, 24* (1993), 1, pp. 109-126
[10] Shuja, S. Z., *et al*., Mixed Convection in a Square Cavity Due to Heat Generating Rectangular Body: Effect of Cavity Exit Port Locations, *International Journal of Numerical Methods for Heat & Fluid-flow*, *10* (2000), 8, pp. 824-841
[11] Manca, O., *et al*., Effect of Heated Wall Position on Mixed Convection in a Channel with an Open Cavity, *Numerical Heat Transfer*, *Part A*, *43* (2003), 3, pp. 259-282
[12] Bahlaoui, A., *et al*., Coupling Between Mixed Convection and Radiation in an Inclined Channel Locally Heated, *J. Mech. Eng*., *55* (2005), 1, pp. 45-57
[13] Saha, S., *et al*., Combined Free and Forced Convection Inside a Two-Dimensional Multiple Ventilated Rectangular Enclosure, *ARPN Journal of Engineering and Applied Sciences*, *1* (2006), 3, pp. 23-35
[14] Manca, O., *et al*., Experimental Investigation of Mixed Convection in a Channel with an Open Cavity, *Experimental heat transfer*, *19* (2006), 1, pp. 53-68
[15] Raji, A., *et al*., Numerical Study of Natural Convection Dominated Hea Transfer in a Ventilated Cavity: Case of foRced Flow Playing Simultaneous Assisting and Opposing Roles, *International Journal of Heat and Fluid-flow*, *29* (2008), 4, pp. 1174-1181
[16] Bahlaoui, A., *et al*., Mixed Convection Cooling Combined with Surface Radiation in a Partitioned Rectangular Cavity, *Energy Conversion and Management*, *50* (2009), 3, pp. 626-635
[17] Bahlaoui, A., *et al*., Height Partition Effect on Combined Mixed Convection and Surface Radiation in a Vented Rectangular Cavity, *Journal of Applied Fluid Mechanics*, *4* (2011), 1, pp. 89-96

[18] Gupta, S. K., *et al*., Investigation of Mixed Convection in a Ventilated Cavity in the Presence of a Heat Conducting Circular Cylinder, *Numer Heat Transfer*, *Part A*, *67* (2015), 1, pp. 52-74
[19] Papanicolaou, E., Jaluria, Y., 'Mixed Convection from an Isolated Heat Source in a Rectangular Enclosure, *Numerical Heat Transfer*, *18* (1991), 4, pp. 427-461
[20] Hsu, T. H., *et al.*, Mixed Convection in a Partially Divided Rectangular Enclosure, *Numerical Heat Transfer*, *Part A Applications*, *31* (1991), 6, pp. 655-683
[21] Raji, A., Hasnaoui, M., Mixed Convection Heat Transfer in a Rectangular Cavity Ventilated and Heated from the Side, *Numerical Heat Transfer*, Part A Applications, *33* (1998), 5, pp. 533-548
[22] Raji, A., Hasnaoui, M., Corrélations en Convection Mixte Dans Des Cavités Ventilées, *Revue généra le de thermique*, *37* (1998), 10, pp. 874-884
[23] Omri., A., Ben Nasrallah, S., Control Volume Finite Element Numerical Simulation of Mixed Convection in an Air-Cooled Cavity, *Numerical Heat Transfer*, *Part A*, *36* (1999), 6, pp. 615-637
[24] Raji, A., Hasnaoui, M., Mixed Convection Heat Transfer in Ventilated Cavities with Opposing and Assisting Flows, *Engineering Computations*, *17* (2000), 5, pp. 556-572
[25] Raji, A., Hasnaoui, M., Combined Mixed Convection and Radiation in Ventilated Cavities, *Eng. Comput.: Int. J. Computer-Aided Eng. Software*, *18* (2001), 7, pp. 922-949
[26] Singh, S., Sharif, M. A. R., Mixed Convective Cooling of a Rectangular Cavity with Inlet and Exit Openings on Differentially Heated Side Walls, *Numerical Heat Transfer*: *Part A: Applications*, *44* (2003), 3, pp. 233-253
[27] Saha, S., *et al.*, Mixed Convection in an Enclosure with Different Inlet and Exit Configurations, *Journal of Applied Fluid Mechanics*, *1* (2008), 1, pp. 78-93
[28] Rahman, *et al.*, Effect of the Presence of a Heat Conducting Horizontal Square Block on Mixed Convection Inside a Vented Square Cavity, *Nonlinear Analysis: Modelling and Control*, *14* (2009), 4, pp. 531-548
[29] Stiriba, Y., *et al.*, Numerical Study of Three-Dimensional Laminar Mixed Convection Past an Open Cavity, *International Journal of Heat and Mass Transfer*, *53* (2010), 21, pp. 4797-4808
[30] Moraga, N. O., Lopez, S. E., Numerical Simulation of Three-Dimensional Mixed Convection in an Air-Cooled Cavity, *Numerical Heat Transfer*, *Part A: Applications*, *45* (2004), 8, pp. 811-824
[31] Doghmi, H., *et al*., Effect of the Inlet Opening on Mixed Convection Inside a 3-D Ventilated Cavity, *Thermal science*, *22* (2018), 6A, pp. 2413-2424
[32] Doghmi, H., *et al*., Three-Dimensional Mixed Convection Heat Transfer in a Partially Heated Ventilated Cavity, *Thermal Science*, *24* (2020), 3B, pp. 1895-1907
[33] Patankar, S. V., *Numerical Heat Transfer and Fluid-flow*, McGraw-Hill,. New York., USA**,** 1980

Paper submitted: May 8, 2019
Paper revised: May 22, 2020
Paper accepted: May 24, 2020